inorganics

MDPI

Review

Keggin Heteropolyacid Salt Catalysts in Oxidation Reactions: A Review

Marcio Jose da Silva *, Alana Alves Rodrigues and Neide Paloma Gonçalves Lopes

Chemistry Department, Federal University of Viçosa, Viçosa 36590-000, Brazil
* Correspondence: silvamj2003@ufv.br

Abstract: Keggin heteropolyacids (HPAs) are metal–oxygen clusters with strong Bronsted acidity. The conversion of HPAs to metal salts can result in Lewis acidity, improving their performance in oxidation reactions. In this review, the main routes for the synthesis of Keggin-type heteropolyacids salts, as well their use as catalysts in oxidation processes of a plethora of substrates, such as monoterpenes, olefins, aldehydes, terpene alcohols, and aromatics, are described. Green reactants such as hydrogen peroxide and molecular oxygen are used as oxidants. These reactions are of interest to several industries because they can be used to produce drugs, additives, fragrances, and fine chemicals. The high efficiency of Keggin HPA with green oxidants contributes to a reduction in the environmental impact of these processes, as preconize the principles of green chemistry. Moreover, Keggin HPAs can be converted to bifunctional catalysts by the modification of their structure, total or partial replacement of their protons with Lewis acid metal cations, or the introduction of these cations into the Keggin anion structure, replacing the addenda atoms (i.e., W and Mo). Aspects linked to the synthesis and characterization of these catalysts are discussed herein, with emphasis on infrared spectroscopy and powder XRD patterns. The most recent advances achieved in the development of catalytic oxidation systems based on Keggin HPA salts are also addressed.

Keywords: Keggin heteropolyacids; solid heteropoly salts; monoterpenes; aromatic aldehydes; olefins; terpene alcohols

check for updates

Citation: da Silva, M.J.; Rodrigues, A.A.; Lopes, N.P.G. Keggin Heteropolyacid Salt Catalysts in Oxidation Reactions: A Review. *Inorganics* **2023**, *11*, 162. https://doi.org/10.3390/inorganics11040162

Academic Editor: Kirill Grzhegorzhevskii

Received: 12 February 2023
Revised: 25 March 2023
Accepted: 27 March 2023
Published: 11 April 2023

Copyright: © 2023 by the authors. Licensee MDPI, Basel, Switzerland. This article is an open access article distributed under the terms and conditions of the Creative Commons Attribution (CC BY) license (https://creativecommons.org/licenses/by/4.0/).

1. Introduction

The development of bifunctional catalysts has attracted attention for economic and environmental reasons [1]. Many bifunctional catalysts have either Lewis or Brønsted acidity functionality, which can promote either acidic or oxidative transformations [2]. Another possible use of the term "bifunctional" is concerning catalysts that can promote hydrogenation and dehydrogenation [3]. Catalysts that can promote reactions for which the main steps require Lewis or Brønsted acid sites are still scarce. Although it is expected that these two types of active sites catalyze different elementary steps within an overall reaction, it is also possible that they participate in the same step.

There are various types of bifunctional catalysts, such as bimetallic catalysts [4]. Normally, these catalysts comprise noble metals as nanoparticles, solid-supported catalysts, and metal oxides [5]. In general, these catalysts have active hydrogenation or oxidation sites [6]. Perovskite oxides are bifunctional catalysts with the general formula ABO_3 or A_2BO_4, where A sites normally represent rare-earth, alkaline-earth, or other large metal cations, while the B sites are transition metal cations. These compounds have been demonstrated to be a class of effective bifunctional catalysts due to their plentiful stoichiometries and crystal structures, as well as multimetal active centers [7]. Bifunctional catalysts frequently combine active metal sites for hydrogenation/dehydrogenation and active acidic sites for protonation/deprotonation steps [8]. Salts containing different counterions can also be used as bifunctional catalysts [9,10].

Keggin heteropolyacids are compounds belonging to the polyoxometalate class that can also be used as bifunctional catalysts [11,12]. Their strong acidity and their structural

properties make them easily modulable. Keggin HPAs are solid metal–oxygen clusters with a high strength of Brønsted acidity, and consequently, they can be used as heterogeneous acid catalysts [13,14]. Although soluble in polar solvents, the exchange of HPA protons with large radium cations makes them heterogeneous catalysts. Moreover, their doping with transition metals results in Lewis acidity or redox potential, which are adequate properties for use in acid-catalyzed or oxidative processes [15–18]. Consequently, Keggin HPA salts have been used in both homogeneous and heterogeneous catalytic reactions [19].

The most widely studied heteropoly catalysts have anions with a typical Keggin structure, as represented by the formula $(XM_{12}O_{40})^{n-}$, where X is the central heteroatom (i.e., Si or P), and tetrahedrally is surrounded with oxygen atoms, which are in octahedral environmental coordination with addenda metal atoms, usually Mo^{6+} or W^{6+} [20].

In this review, various procedures to prepare Keggin HPA salts are addressed, with an emphasis on those involving unsupported catalysts and a focus on lacunar heteropoly salts, transition metal cation-exchanged salts, and transition metal-doped salts. Beyond synthesis and characterization, special attention is dedicated to describing their applications as catalysts in oxidation and acid-catalyzed reactions.

2. Main Routes to Synthesize POMs Salts

2.1. Synthesis of Metal-Exchanged Phosphotungstic, Phosphomolybdic, and Silicotungstic Acid Salts

Transition metal cation-exchanged salts can be easily synthesized starting from the metathesis of Keggin HPA solution with another solution containing the metal chloride with adequate stoichiometry, according to literature (Scheme 1) [21,22]. In this process, the metal chloride solution is slowly dropped into the Keggin HPA solution; afterwards, the mixture is heated to release water and HCl, resulting in a solid salt, which is dried in an oven at 423 K.

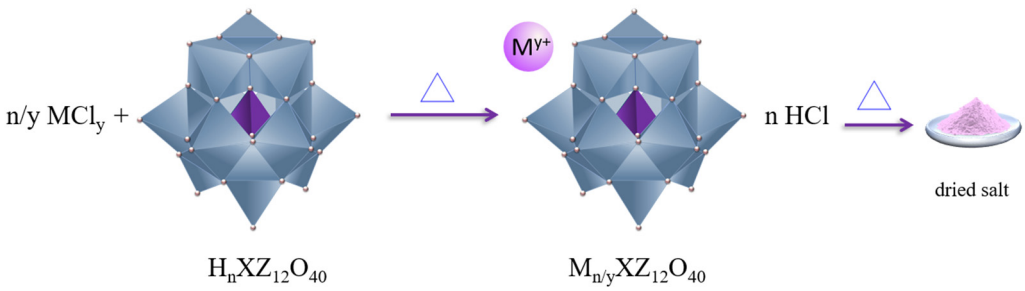

n = 3 or 4; y = nox cation M; X = P or Si, Z = W or Mo

Scheme 1. Synthesis of metal-exchanged phosphotungstic, phosphomolybdic, and silicotungstic acid salts.

When the metal cation has large ionic radium such as K^+, Rb^+, or Cs^+ ions, the metal-exchanged Keggin HPA salt is precipitated into the reaction solution. Other cations such as ammonium and tetrabutylammonium have been widely used to synthesize the insoluble HPAs [23]. Consequently, when the HPA is insoluble, it is separated through a filtration step [24]. However, if the metal cation has an ionic radium smaller than 1.3 Angstroms, the HPA salt is water-soluble; therefore, separation requires the vaporization of the solvent [25,26].

Figure 1 shows the yield achieved in the syntheses of the metal-exchanged silicotungstic acid salts [27]. In almost all cases, high yields were attained, demonstrating that this is an attractive route to obtain these HPA salts.

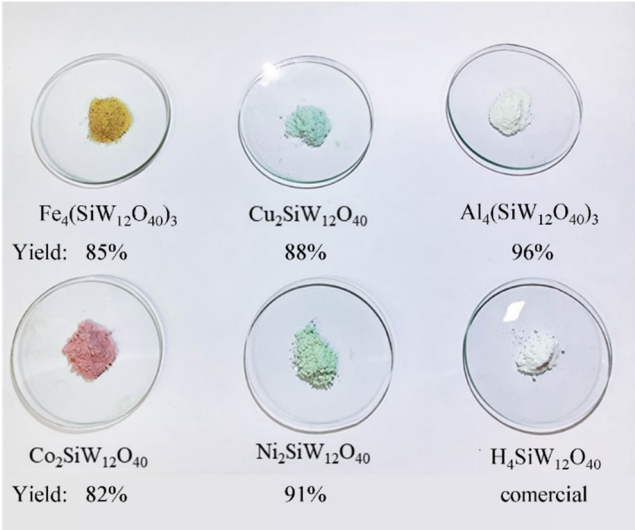

Figure 1. The yield of synthesis of the metal-exchanged silicotungstic acid salts [27].

2.2. Synthesis of Phosphotungstic, Phosphomolybdic, and Silicotungstic Acids Lacunar Salts

Lacunar Keggin anions are obtained from hydrolyzes of the pristine Keggin HPAs or their salts [28]. The hydrolysis reaction occurs when a $NaHCO_3$ solution is added to the HPA solution. This is a key step because the pH control is straightly linked to the number of MO units removed from the Keggin anions (Scheme 2).

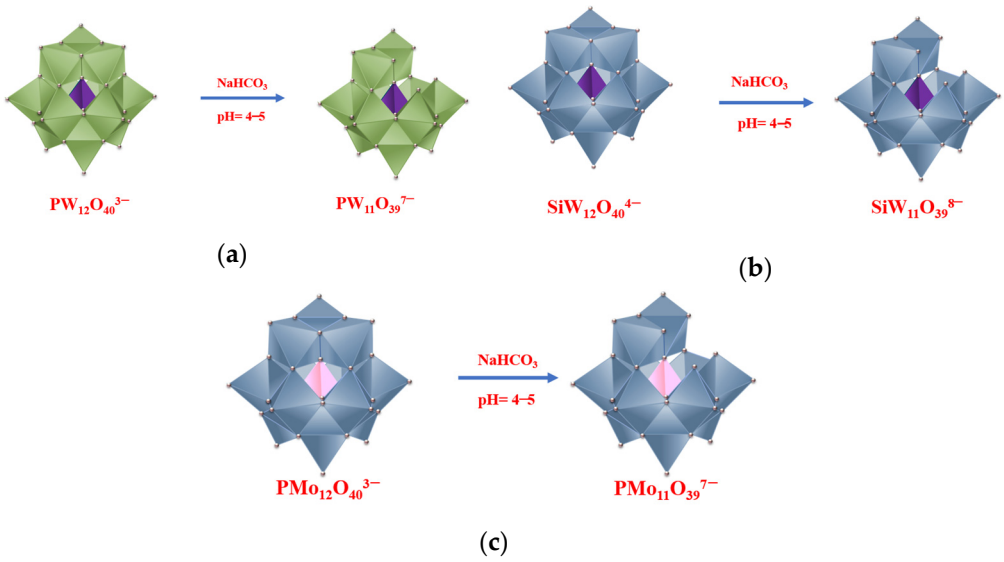

Scheme 2. Synthesis of phosphotungstic (**a**), silicotungstic (**b**), and phosphomolybdic acid (**c**) lacunar salts.

However, this synthesis route requires the presence of the pristine HPA or their salt, which has a saturated anion. Alternatively, it is possible to obtain the Keggin HPA and afterwards their lacunar salt through the one–pot procedure. To do it, solutions containing the synthesis precursors in stoichiometry amount should be gently mixed and then the pH should be adjusted with $NaHCO_3$ solution, resulting in the lacunar heteropolyanion salt. Schemes 3–5 show these procedures.

It is noteworthy that the lacunar HPAs can be obtained as soluble or insoluble salts, depending on the ionic radius of the metal cation that replaces the protons [29,30].

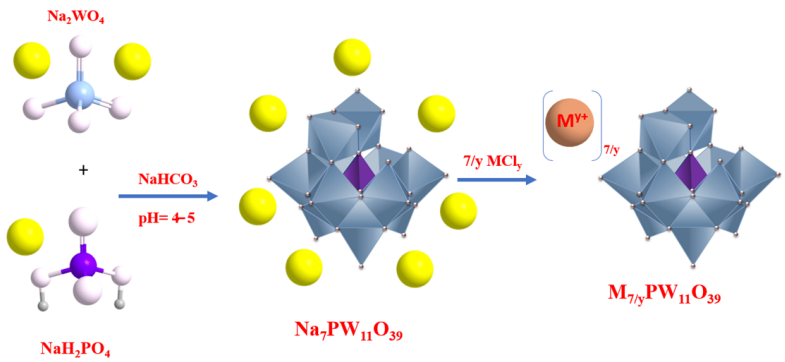

Scheme 3. One–pot synthesis of phosphotungstic acid lacunar salt.

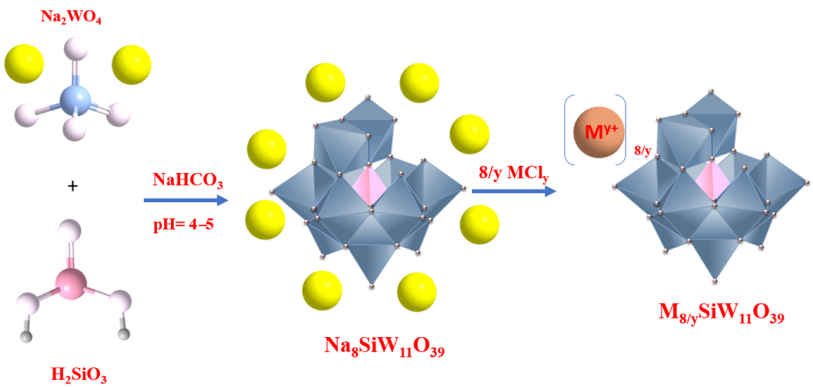

Scheme 4. One–step synthesis of silicotungstic acid lacunar salt.

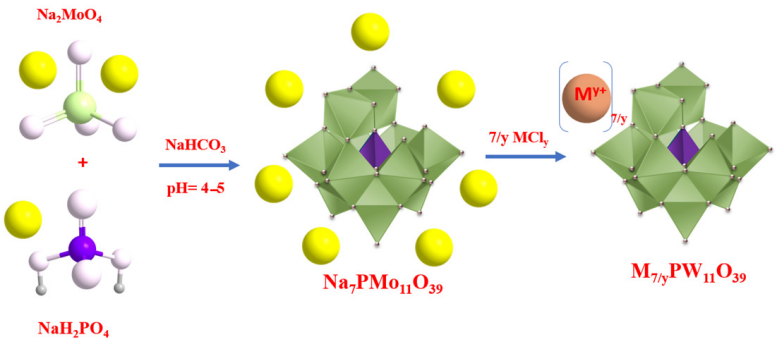

Scheme 5. One–step synthesis of phosphomolybdic acid lacunar salt.

2.3. Synthesis of Metal-Substituted Lacunar HPA Salts

The doping of lacunar salts with transition metal cations is an efficient strategy to convert these salts into highly active catalysts in oxidation reactions with hydrogen peroxide. Copper, nickel, manganese, vanadium, zinc, and iron are the most common dopants [31,32]. Scheme 6 describes how converting the saturated Keggin heteropolyanion to a lacunar anion and posteriorly to a metal-doped anion.

Charge balancing is done by the counter-ion, which was omitted for clarity. Once more, the solubility of these salts may vary according to the size of the cation. The pH control is a key step herein. An excessive increase in the pH may promote successive hydrolysis of the Keggin anion, and di-or tri-lacunar species can be obtained.

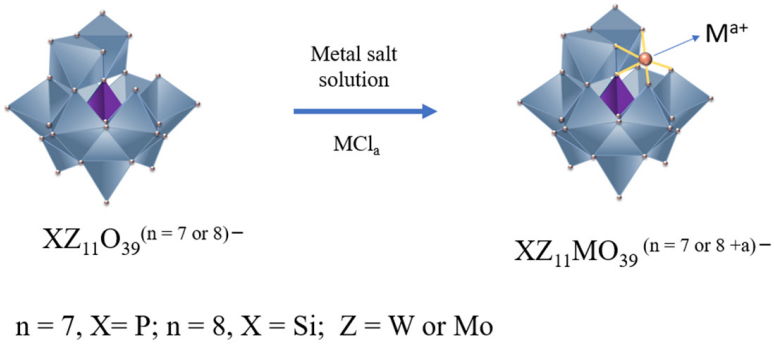

Scheme 6. Synthesis of metal-doped phosphotungstate, phosphomolybdate, and silicotungstate heteropolyanions.

3. Characterization Techniques of Keggin HPA Salts

There are several techniques used to characterize Keggin HPA salts, however, we will emphasize only those more frequently used [33]. Most results were previously obtained by us and the references were adequately cited [26–30,34,35].

3.1. Infrared Spectroscopy

Infrared spectroscopy gives information on the primary structure of Keggin HPAs (i.e., heteropolyanion) [34]. The fingerprint region shows the typical absorption bands assigned to the vibration of chemical bonds involving Si-O, W-O$_b$-W, W-O$_c$-W, and W = O$_d$ atoms. The subscript distinguishes the oxygen atoms in the function of the position occupied in the heteropolyanion [27].

The profile of infrared spectra of silicotungstate anion remained intact after the protons exchange with metal cations (Figure 2). This indicates that the Keggin structure was preserved after the synthesis of heteropoly salts.

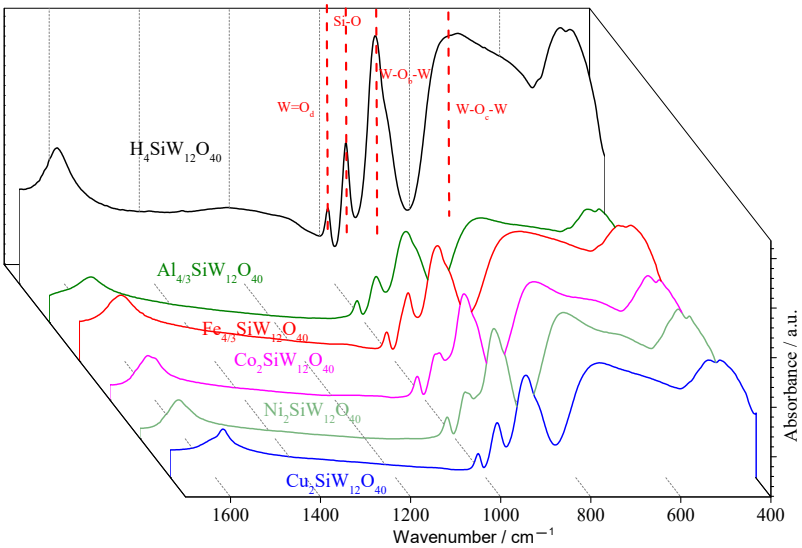

Figure 2. Infrared spectra of metal-exchanged silicotungstic acid salts (adapted from ref. [27]).

Figure 3 shows a comparison of infrared spectra of pristine HPAs (i.e., $H_3PW_{12}O_{40}$, $H_3PMo_{12}O_{40}$, and $H_4SiW_{12}O_{40}$) and their aluminium-exchanged salts.

The main absorption bands assigned to the vibrations of chemical bonds of Keggin anion seen in the infrared spectra of pristine HPAs were also observed in the spectra of aluminium salts.

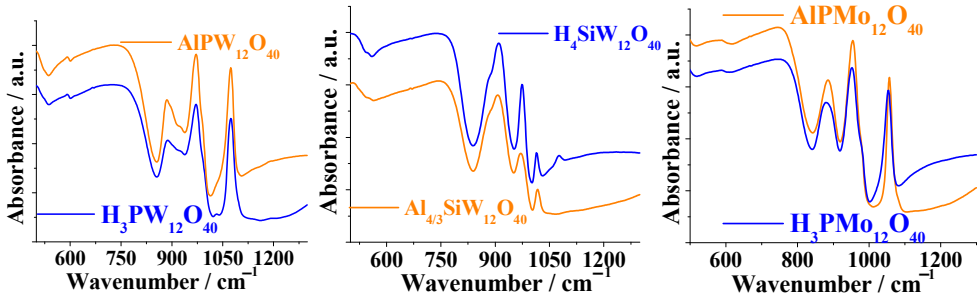

Figure 3. Infrared spectra of phosphotungstic, silicotungstic, and phosphomolybdic acids and their aluminium-exchanged salts (adapted from refs. [34,35]).

The same comparison was also performed with infrared spectra of iron heteropoly salts (Figure 4).

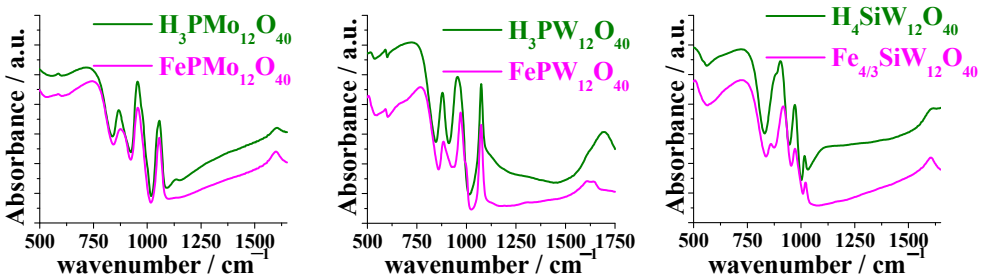

Figure 4. Infrared spectra of phosphotungstic, silicotungstic, and phosphomolybdic acid and their iron-exchanged salts (adapted from refs. [34,35]).

As verified in the infrared spectra of aluminium-exchanged salts, the Keggin anion structure was preserved after the synthesis of the iron-exchanged salts [36].

3.2. Powder X-rays Diffraction Patterns

While infrared spectroscopy provides information about the primary structure of Keggin HPAs (i.e., heteropolyanion), the powder XRD patterns give information on the secondary structure, which comprises the tridimensional arrangement of Keggin heteropolyanions surrounded by cations (i.e., hydronium, di-hydronium, metals) and water molecules [34–38]. Figure 5 displays the primary, secondary, and tertiary structures of the metal-doped heteropoly salts.

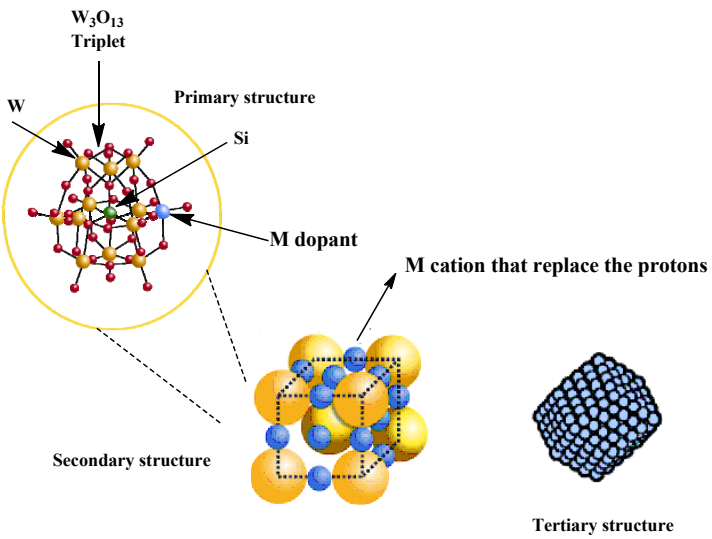

Figure 5. Primary, secondary, and tertiary structures of Keggin anion.

The Bragg equation describes the relation between interplanar distance "d" and scattering 2 θ angles.

$$\sin \theta = n \lambda / 2d \quad (1)$$

An increase in metal cation radium led to a greater "d" value, consequently, it is expected that 2 θ angle values become smaller than scattering angles of pristine HPA. However, this distance is impacted too by the water molecules. Therefore, ionic radium is not the only aspect to be considered.

Figure 6 presents the powder XRD patterns of silicotungstic acid and their metal-exchanged cations. Diffractograms of the metal cation-exchanged silicotungstic acid salts have some typical diffraction peaks. The main appears at low 2 θ angles (i.e., 6° to 9°), 15° and 30° 2 θ angles. In particular, the diffractograms of trivalent cation salts (i.e., Fe^{3+}, and Al^{3+} ions) have more well-defined and more intense diffraction peaks. The differences observed between XRD patterns of silicotungstic acid, and their metal-exchanged salts can be a consequence of different hydration levels (Table 1), as well as the different sizes of ionic radium of metal cations.

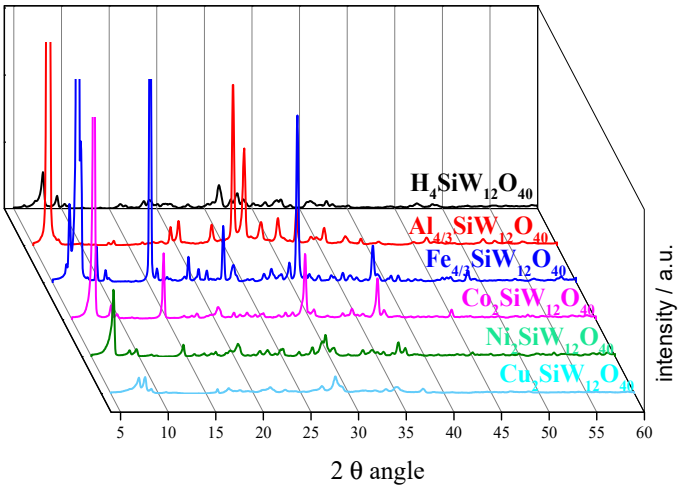

Figure 6. Powder XRD patterns of silicotungstic acid and their metal-exchanged cations (adapted from ref. [27]).

Table 1. Hydration water molecules were determined through thermal analysis (DTG) [27].

Catalyst	Water/Catalyst mol
$H_4SiW_{12}O_{40}$	11
$Ni_2SiW_{12}O_{40}$	7
$Cu_2SiW_{12}O_{40}$	7
$Co_2SiW_{12}O_{40}$	10
$Fe_{4/3}SiW_{12}O_{40}$	13
$Al_{4/3}SiW_{12}O_{40}$	8

The comparison of powder XRD patterns of tungsten HPAs with their aluminium salts showed that at 2 θ angles greater than 50°, the diffractogram of acids displays diffraction lines present more intensity than their salts. This did not occur with molybdenum HPAs. Moreover, diffractograms of tungsten heteropoly acids had a more significant peak number. The different ionic radium of W^{6+} and Mo^{6+} cations and the distinct hydration levels affect the diffraction patterns of these acids and their heteropoly salts. Moreover, Al^{3+} and H_3O^+ or $H_5O_2^+$ have ionic radium with different sizes, triggering thus change in the diffraction patterns. Although XRD patterns can give important information about the secondary structure, it is unable to distinguish the different isomeric structures of the Keggin anion. However, due to the difficulty to isolate Keggin isomers and evaluate separately their catalytic activity, most of the time these aspects are not addressed. Figure 7

shows a comparison between the powder XRD patterns of pristine HPAs (i.e., $H_3PW_{12}O_{40}$, $H_3PMo_{12}O_{40}$, and $H_4SiW_{12}O_{40}$) and their aluminium-exchanged salts.

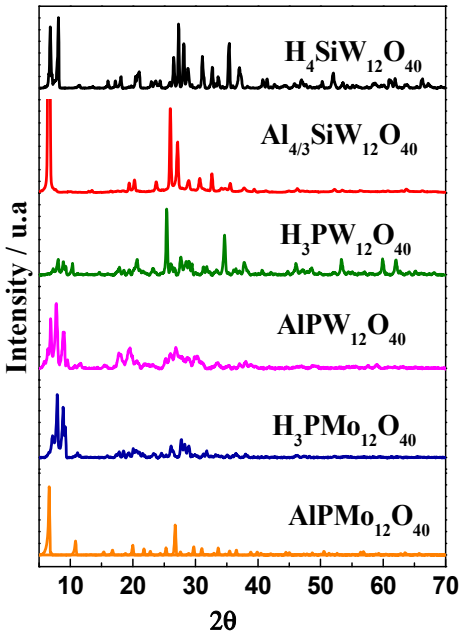

Figure 7. Powder XRD patterns of phosphotungstic, silicotungstic, and phosphomolybdic acid and their aluminium-exchanged salts (adapted from refs. [34,35]).

3.3. Acidity Properties

Potentiometric titration is a technique that allows estimating the number of acid sites, from the plateau region of titration curves. Moreover, it can be determined from the titration curve's first-derived curve. The strength of acidic sites is estimated from the initial value of electrode potential (Ei). They are classified as follows: $E > 100$ mV (very strong sites), $0 < E < 100$ mV (strong sites), $-100 < E < 0$ (weak sites), and $E < -100$ mV (very weak sites) [38]. However, this technique did not distinguish the nature of acid sites (i.e., Lewis or Brønsted).

It is important to note that although the chemical formulae of salts suggest that there is no proton, a residual amount remains still. Moreover, the literature describes that Lewis acid metal cations can react with the hydration water molecules giving H_3O^+ ions, which consume *n*-butylamine. Moreover, the transition metal cations can themself react with the nitrogen of the base [27]. Therefore, the titrant *n*-butylamine is still consumed when the salts are titrated.

Figure 8 displays the potentiometric titration curves of silicotungstic acid and their silicotungstate salts. All the salts presented very strong acid sites (Ei > 100 mV). However, the profile of M^{2+} and M^{3+} cation salts titration curves differed. Typically, the titration of $Al_{4/3}SiW_{12}O_{40}$ and $Fe_{4/3}SiW_{12}O_{40}$ solutions gave curves with a well-defined plateau, likewise the pristine $H_4SiW_{12}O_{40}$. Conversely, the titration of $Cu_2SiW_{12}O_{40}$, $Ni_2SiW_{12}O_{40}$, and $Co_2SiW_{12}O_{40}$ solutions resulted in curves with two plateaus. The profile of these three last curves suggests that there are acid sites with distinct strengths of acidity [27].

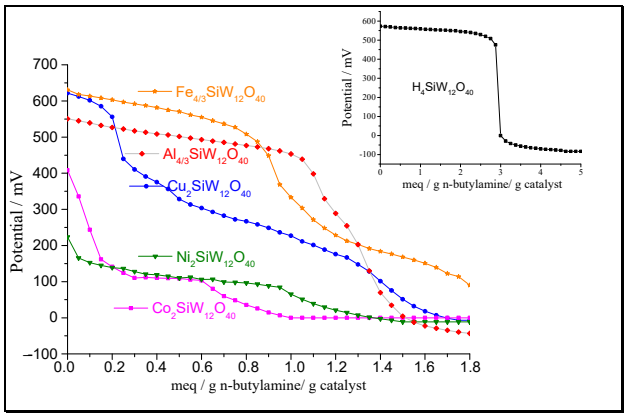

Figure 8. Potentiometric titration curves of silicotungstic acid and their metal-exchanged salts (adapted from ref. [27]).

4. Keggin HPA Salts as Catalysts in Oxidation Reactions

Keggin HPAs such as phosphomolybdic acid are active in oxidation reactions even in the absence of metal as countercations or dopants. However, depending on the selected substrate (i.e., aldehydes, alcohols, olefins), the presence of cation metal may trigger a synergism and increase its efficiency. From a practical viewpoint, most of the reactions require an initial screening to select the most active Keggin HPA salt. The catalytic activity of HPA salts can be linked to the electronic aspects, which are modified in the presence of metal cations in determined positions.

Aluminium or copper salts of the phosphotungstic and silicotungstic acids were synthesized and used as catalysts in 2-methoxynaphthalene acylation [39]. These catalysts were compared and the main results are in Figure 9.

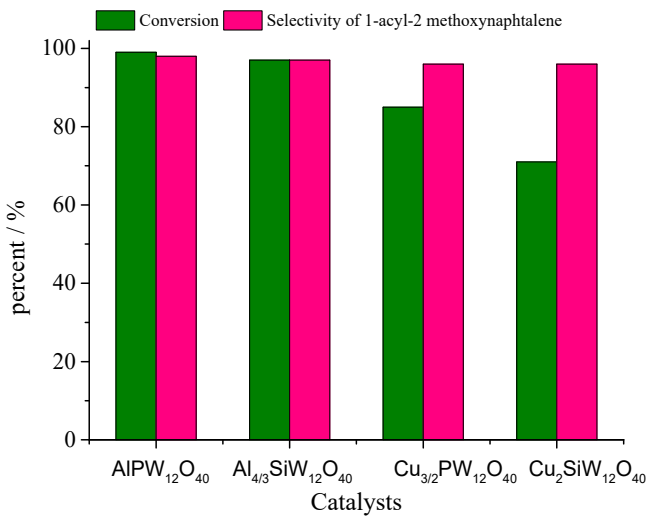

Figure 9. 2-Methoxynaphthalene acylation using aluminium or copper salts of phosphotungstic silicotungstic acids as catalysts (adapted from ref. [39]) [a]. [a] Reaction conditions: time: 65 min, temperature: 373 K.

The highest conversion and selectivity toward acyl methoxy naphthalene were reached in the $AlPW_{12}O_{40}$-catalyzed reaction. Keggin HPA iron salts were evaluated in etherification reactions of β-pinene with alkyl alcohols [34]. Salts of three Keggin HPAs were synthesized containing aluminium or transition metal cations. Among them, $FePW_{12}O_{40}$ was the most efficient catalyst converting the β-pinene mainly to α-terpinyl alkyl ether (Scheme 7). The secondary products were fenchyl and bornyl alkyl ethers resulting from the

carbon skeletal rearrangement reaction of β-pinene followed by the nucleophilic addition of alkyl alcohol.

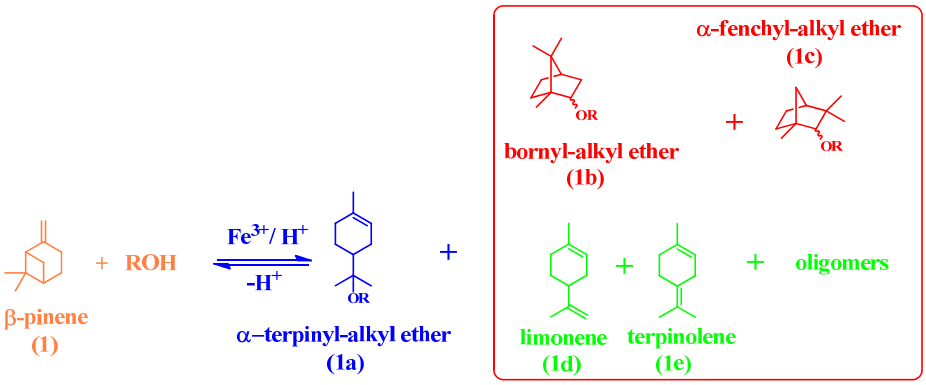

Scheme 7. The main products of the iron phosphotungstate-catalyzed reactions of β-pinene with alkyl alcohol (adapted from ref. [34]).

Those authors compared the effect of the Keggin anion on the catalytic activity of iron salts in the reaction of β-pinene with methyl alcohol. Figure 10 displays the main results.

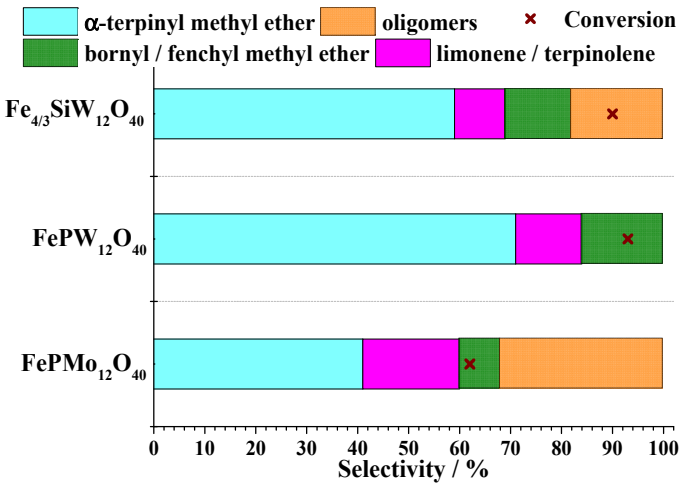

Figure 10. Impacts of Keggin anion on the conversion and selectivity of Keggin HPA iron salts phosphotungstate-catalyzed reaction of β-pinene with methyl alcohol (adapted from ref. [34]) [a]. [a] Reaction conditions: β-pinene (3.8 mmol), CH_3OH (14.3 mL), temperature (333 K), catalyst (0.50 mol%), volume (10 mL).

Although the reactions in the presence of iron silicotungstate or phosphotungstate have achieved almost the same conversion, this last was the most selective toward the goal product (i.e., α-terpinyl methyl ether). In Figure 11, the activity of $FePW_{12}O_{40}$ was compared to the other Lewis acid metal cations (i.e., Cu^{2+} and Al^{3+}).

The highest activity of the $FePW_{12}O_{40}$ catalyst was attributed to its highest Lewis acidity, which promotes the reaction of carbon skeletal of β-pinene and gives the α-terpinyl carbocation, the most probable reaction intermediate.

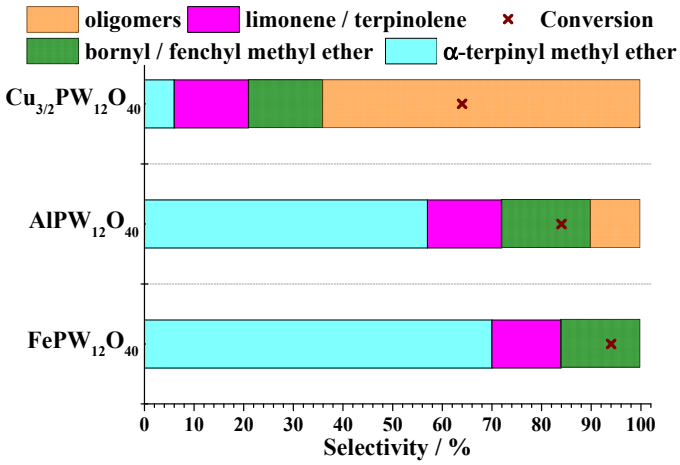

Figure 11. Impacts of metal cation on the conversion and selectivity of phosphotungstate-catalyzed reaction of β-pinene with methyl alcohol (adapted from ref. [34]) [a]. [a] Reaction conditions: β-pinene (3.8 mmol), CH_3OH (14.3 mL), temperature (333 K), catalyst (0.50 mol%), volume (10 mL).

The impact of the size of the carbon chain was also evaluated in reactions with C1-C4 alcohols and β-pinene (Scheme 8) [34].

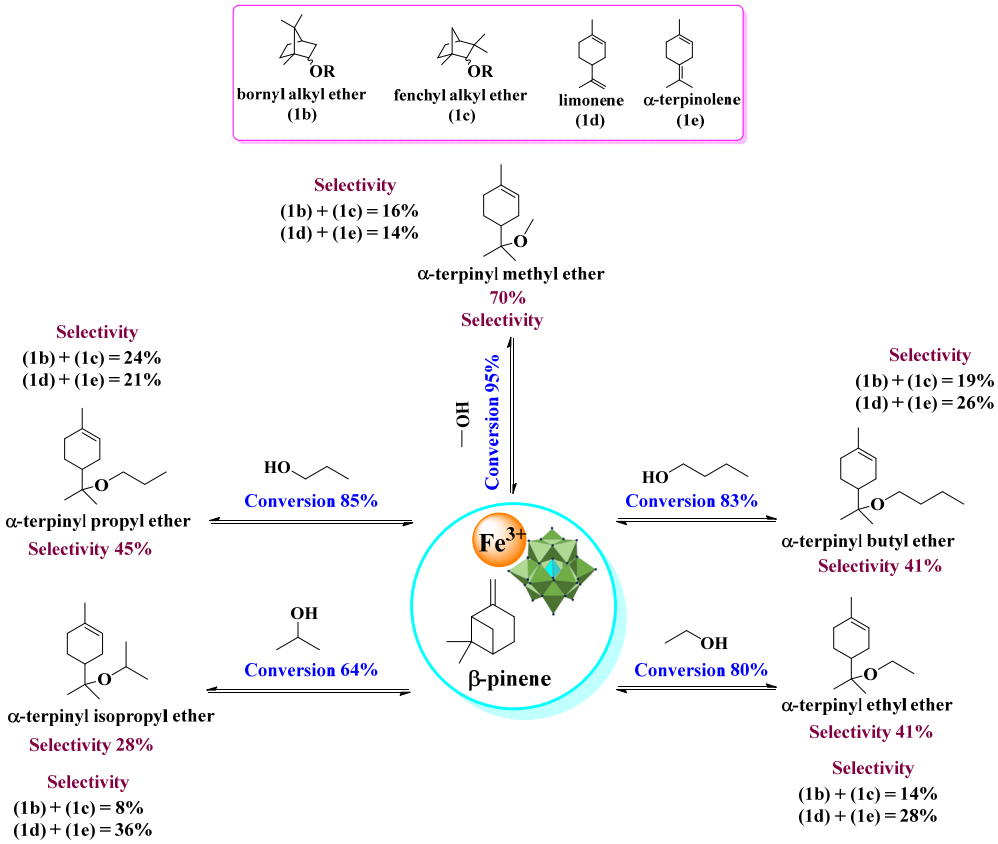

Scheme 8. $FePW_{12}O_{40}$-catalyzed-etherification of β-pinene with different alkyl alcohols (adapted from ref. [34]).

An increase in the carbon chain size and steric hindrance of the hydroxyl group may leave to a lower conversion and ether selectivity. However, herein, high conversions were attained regardless of alcohol. The conversions achieved in the reactions with methyl ethyl, propyl and butyl alcohols were 95%, 80,%, 85%, and 83%, respectively. Therefore, although these three last conversions have been lower than reached in the reaction of methyl alcohol,

this effect was less pronounced herein. Conversely, the selectivity to α-terpinyl alkyl ether was 70%, 41%, 45%, and 41%, in the reactions with methyl ethyl, propyl and butyl alcohols, respectively. Thus, it suggests that only methyl alcohol shows a high selectivity. The other alcohols, regardless of the size of the carbon chain have similar reactivity. Due to the steric hindrance, isopropyl alcohol was the less reactive, reaching the lowest conversion and ether selectivity [34].

Aluminium heteropoly salts were evaluated in oxidation reactions of camphene, another monoterpene [35]. In that work, the aluminium silicotungstate salt (i.e., $Al_{4/3}SiW_{12}O_{40}$) was the most active and selective toward the formation of borneol. Nonetheless, the novelty was the formation of two novel products: 1-(3-(2-hydroxy propan-2-yl) cyclopentyl) ethan-1-one, and 3-(3-hydroxy cyclopentyl)-3-methyl butan-2-one. Scheme 9 shows the conversion and selectivity achieved in the presence of aluminium-exchanged Keggin HPAs salts.

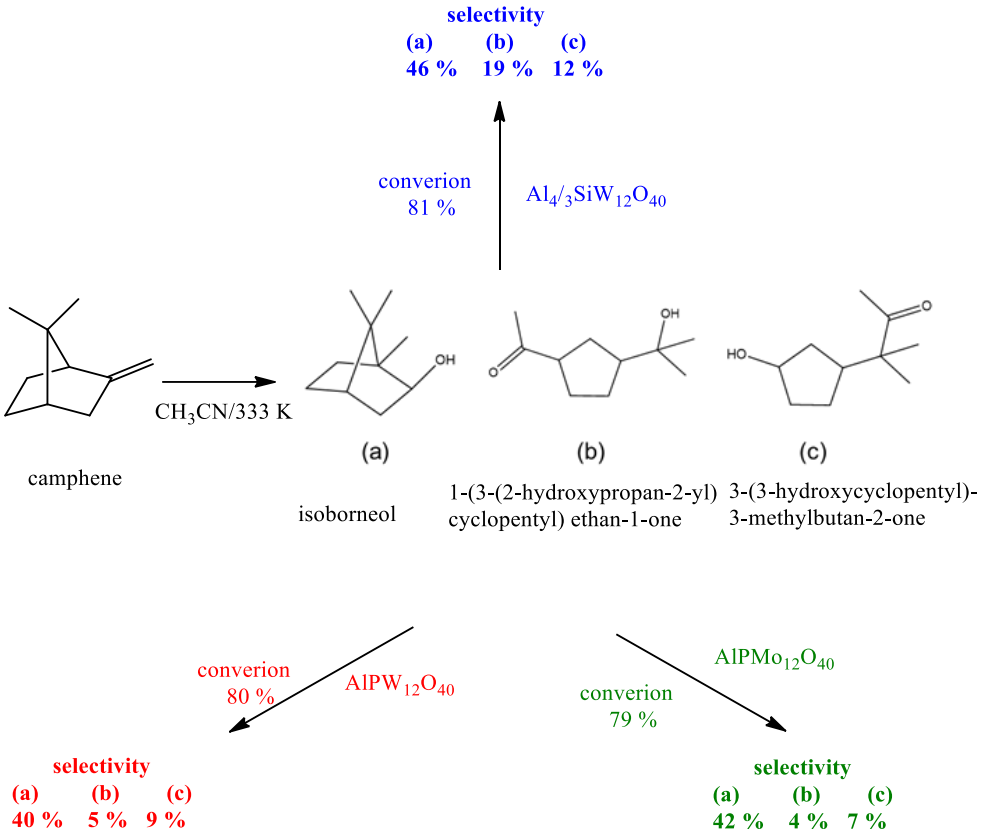

Scheme 9. Effect of Keggin anion on conversion and selectivity of Al^{3+} heteropoly salts-catalyzed camphene oxidation by hydrogen peroxide in CH_3CN (adapted from ref. [35]).

Remarkably, the $Al_{4/3}SiW_{12}O_{40}$ salt provided the highest selectivity toward the two novel products. The authors attributed this to the greatest Lewis acidity of the catalyst. After carrying out reactions with $Al(NO_3)_3$ salt and $H_{43}SiW_{12}O_{40}$ acid, those authors demonstrated that a synergism occurs between the Al^{3+} cation and silicotungstate anion [35].

Metal-exchanged silicotungstic acid salts were evaluated as catalysts in furfural oxidation reactions with hydrogen peroxide [27]. Furfural-derived products such as furfuryl ester and dimethyl acetal are valuable compounds for bioadditives formulation.

In this one-pot process, furfural was selectively oxidized to acid and esterified in the presence of methyl alcohol (Scheme 10). Copper silicotungstate was the most effective catalyst, which was more efficient than other Lewis's acid catalysts also tested such as aluminium or iron silicotungstate. Therefore, it can be concluded that different from verified in the reactions of carbon skeletal rearrangement followed by the oxidation of camphene (see ref. [33]), where the Lewis acidity was a key aspect to explain the highest

activity of Al^{3+} phosphotungstate, herein other aspects can be also important. For instance, the nature of heteropolyanion plays an essential role in these reactions.

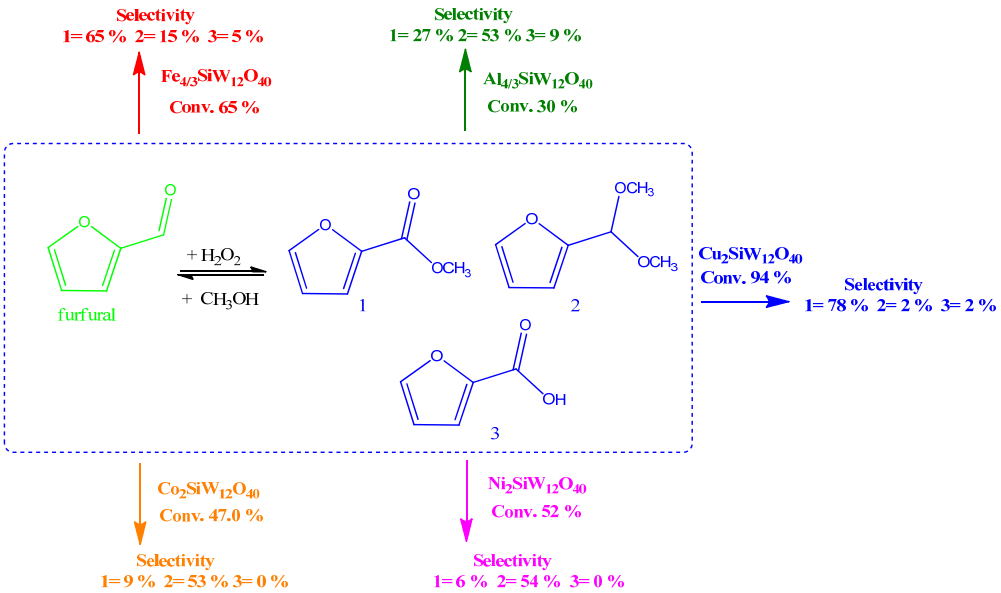

Scheme 10. Metal-exchanged silicotungstic acid salts-catalyzed reactions of furfural with hydrogen peroxide (adapted from ref. [26]) [a]. [a] Reaction conditions: furfural (2.5 mmol), CH_3OH (9.4 mL, 231 mmol), H_2O_2 (5.0 mmol), temperature (323 K), catalyst (1.0 mol%, 25.0 µmol), volume (10 mL).

The $Cu_2SiW_{12}O_{40}$-catalyzed oxidative esterification of furfural was carried out with hydrogen peroxide in the presence of different alkyl alcohols (Scheme 11).

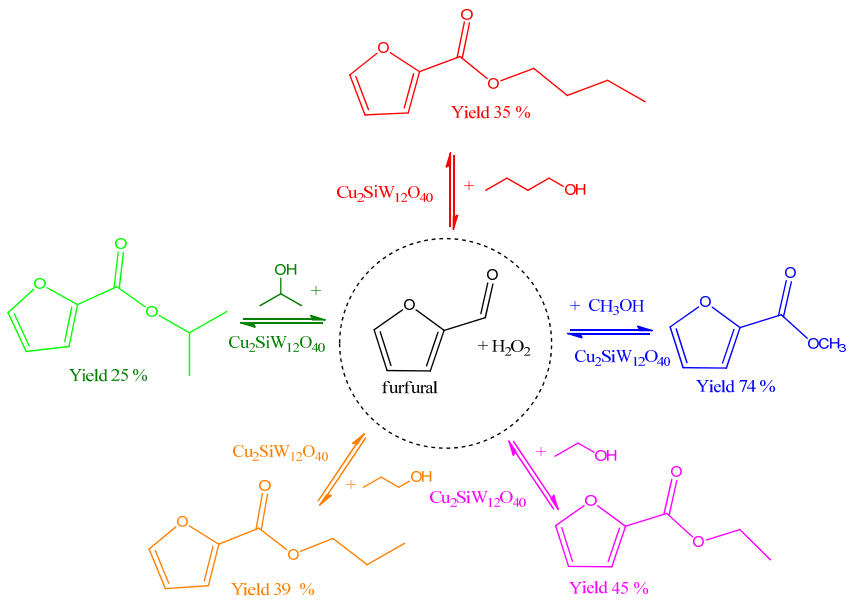

Scheme 11. Impact of alcohol on the $Cu_2SiW_{12}O_{40}$-catalyzed oxidative esterification of furfural with hydrogen peroxide (adapted from ref. [27]) [a]. [a] Reaction condition: furfural (2.5 mmol), alky alcohol (9.4 mL), H_2O_2 (5.0 mmol), temperature (323 K), catalyst (1.0 mol%, 25.0 µmol), reaction volume (10 mL).

Scheme 11 shows the yield only to alkyl esters. An increase in the size of the carbon chain of alcohol harmed ester yield. This may be a consequence of hydrophobic forces, which increase with the size of the carbon chain.

Although all salts evaluated have been soluble in the reaction medium, a recycling process was developed to recover and reuse the catalyst (Figure 12).

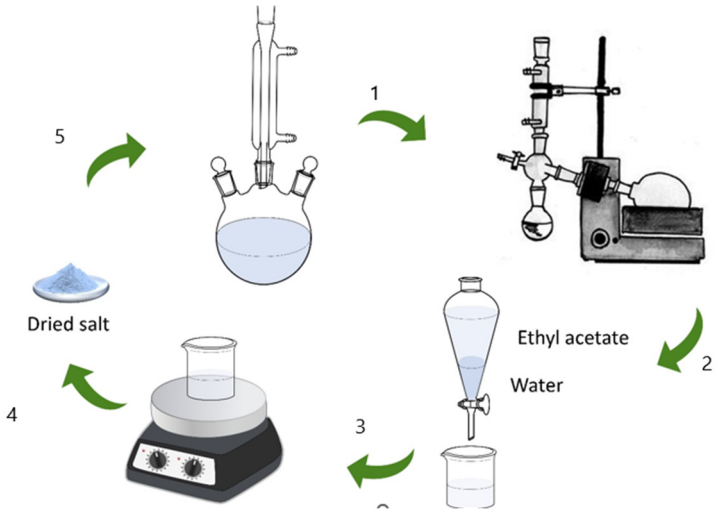

Figure 12. Procedure to recover and reuse the soluble catalyst [27].

After the catalytic run, the solvent of the reaction is removed in a rotatory evaporator, and the neat remaining is extracted with a mixture of water/ethyl acetate. The Keggin HPA salt catalyst is soluble in water, which is evaporated, giving the solid catalyst. Afterwards, it is weighted and used in another catalytic cycle. Table 2 shows the conversion and recovery rates obtained after the successive cycles of recovery/reuse.

Table 2. The recovery rates and conversions achieved in the reuse of $Cu_2SiW_{12}O_{40}$ catalyst in oxidative esterification reactions of furfural with hydrogen peroxide [27].

Cycle	Catalyst Recovery (%)	Conversion (%)
1	92	97
2	92	93
3	92	92
4	91	94

In oxidation reactions with molecular oxygen, molybdenum HPAs have been more active than tungsten. Cobalt cations-doped catalysts have been active in oxidation reactions [30,40]. Swericka et al. studied the effect of the Co position within the Keggin anion of the catalysts, using cyclooctane as a model molecule [41].

Scheme 12 shows the main results achieved in these reactions. Cyclooctane was preferentially oxidized to cyclooctanol, cyclooctenone, and cyclooctane peroxide, regardless of the catalyst. However, the oxygenates yield was higher in the reactions carried out in the presence of molybdenum HPA or their salts if compared to the tungsten catalysts. The reactions with cobalt as a counterion or as a dopant of heteropolyanion achieved the same oxygenate yields. The same happened with tungsten salts that had Co as a counterion. However, while phosphomolybdic acid reached the same yield as their cobalt salts, the phosphotungstic acid-catalyzed oxidation of cyclooctane achieved the lowest oxygenate yield [41].

Lacunar salts have been effective catalysts in oxidation reactions of terpene alcohols with hydrogen peroxide, even as undoped salts. Vilanculo et al. explored these catalysts in various reactions like these. Scheme 13 displays the main products obtained in $Na_7PW_{11}O_{39}$-catalyzed linalool oxidation with hydrogen peroxide [30].

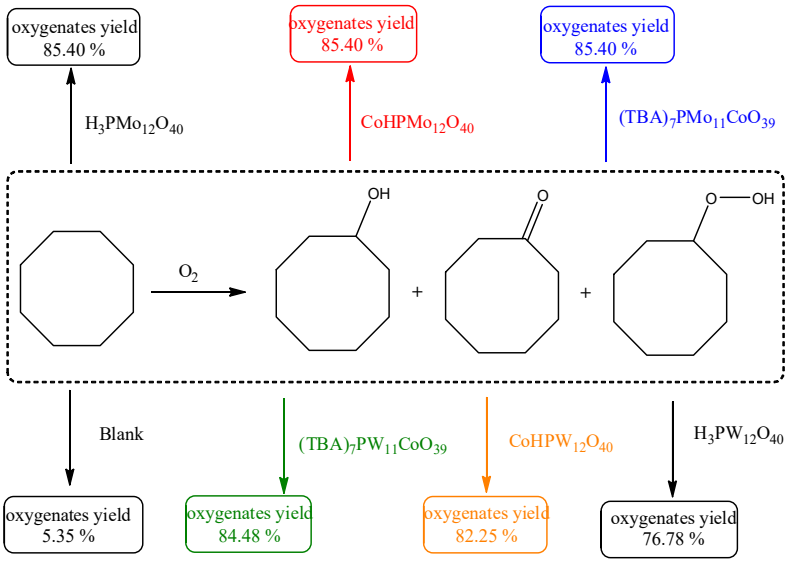

Scheme 12. Oxidation of cyclooctane with molecular oxygen in the presence of phosphotungstic or phosphomolybdic acids or their cobalt salts (adapted from ref. [41]).

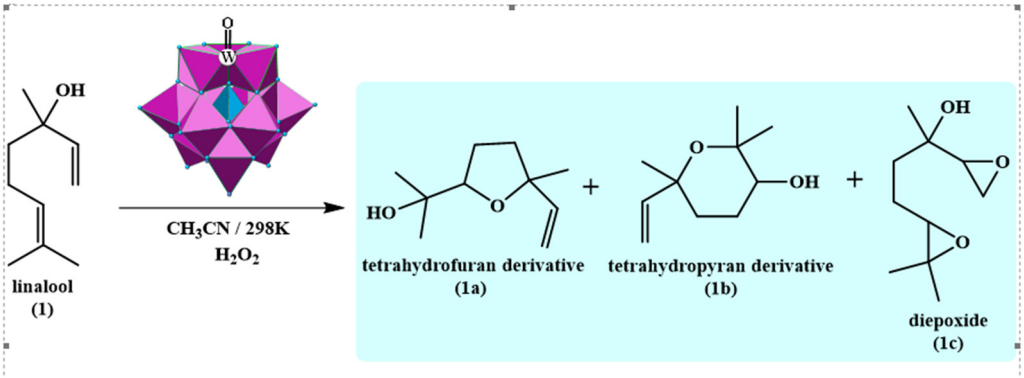

Scheme 13. Main products of $Na_7PW_{11}O_{39}$-catalyzed linalool oxidation with hydrogen peroxide (adapted from ref. [30]).

Linalool is an unsaturated tertiary alcohol, which may be epoxidized generating mono or diepoxides. However, herein it was cyclized generating furane and pyrane derived, which were isolated and spectroscopically characterized [30]. Those authors assessed the effect of Keggin heteropolyanion in this reaction and the main results are shown in Figure 13.

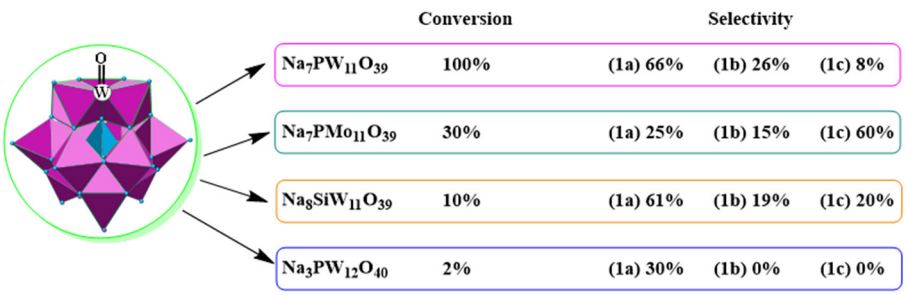

Figure 13. Impact of heteropolyanion on the efficiency of Keggin HPA sodium salts (adapted from ref. [30]).

The saturated salt $Na_3PW_{12}O_{40}$ was inactive, reinforcing that the presence of vacancy in the anion is an essential aspect of the activity of these catalysts. The lacunar tungsten

sodium salt catalysts were more efficient than molybdenum, being the lacunar sodium phosphotungstate salt the most active, achieving the highest conversion and selectivity toward furan-derived (Figure 13).

Da Silva et al. investigated the activity of these sodium HPA salts in oxidation reactions of nerol, an allylic terpene alcohol. Hydrogen peroxide was the oxidant and acetonitrile was the solvent [26]. Figure 14 describes the results obtained using different sodium salts, the main products, and a probable reaction pathway.

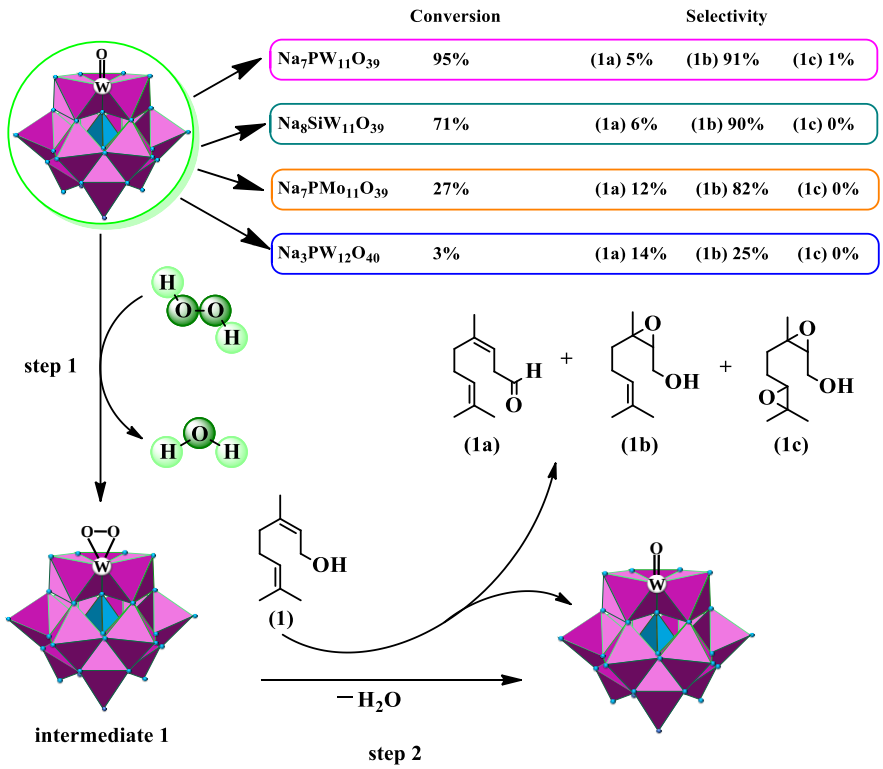

Figure 14. Impact of heteropolyanion on the efficiency of Keggin HPA sodium salts, main oxidation products of nerol a probable reaction pathway (adapted from ref. [26]).

As verified in the linalool oxidation, lacunar tungsten salt catalysts were more efficient than molybdenum ones. Again, saturated salt was inactive. Different from linalool, which undergoes a cyclization reaction, the nerol was preferentially epoxidized giving monoepoxide as the main product, diepoxide, and aldehyde as secondary products [26,30]. Those authors demonstrated that this epoxidation of allylic alcohols is a hydroxy group-assisted reaction.

Figure 15 describes the probable reaction pathway. According to this proposal, the lacunar heteropolyanion is peroxidized, generating intermediate 1, which transfers the oxygen atom to the substrate, releasing water and the oxidation product [26,30].

Transition metal cations-doped silicotungstic acid salts were evaluated as catalysts in oxidation reactions with hydrogen peroxide [42]. In these reactions, borneol, a terpene alcohol was selectively converted to camphor, a product with wide application in the pharmaceutic and fragrancies industries. Figure 15 exhibits the main results achieved in reactions where the vacancy of lacunar salt $K_8SiW_{11}O_{39}$ was filled with a transition metal cation.

Only the nickel and iron-doped potassium silicotungstate salts achieved a camphor yield equal or superior to that reached by the lacunar potassium silicotungstate salt. However, while the $K_8SiW_{11}O_{39}$-catalyzed reaction attained the maximum conversion after 2 h of reaction, in the presence of the $K_6SiW_{11}NiO_{39}$ catalyst it was achieved within the first hour of reaction. Interestingly, when the copper acted as a countercation of silico-

tungstate salt, it was the best catalyst in furfural oxidation [27]. Herein, as a dopant, the copper was the worst catalyst, achieving the lowest camphor yield on the borneol oxidation (Figure 14) [42].

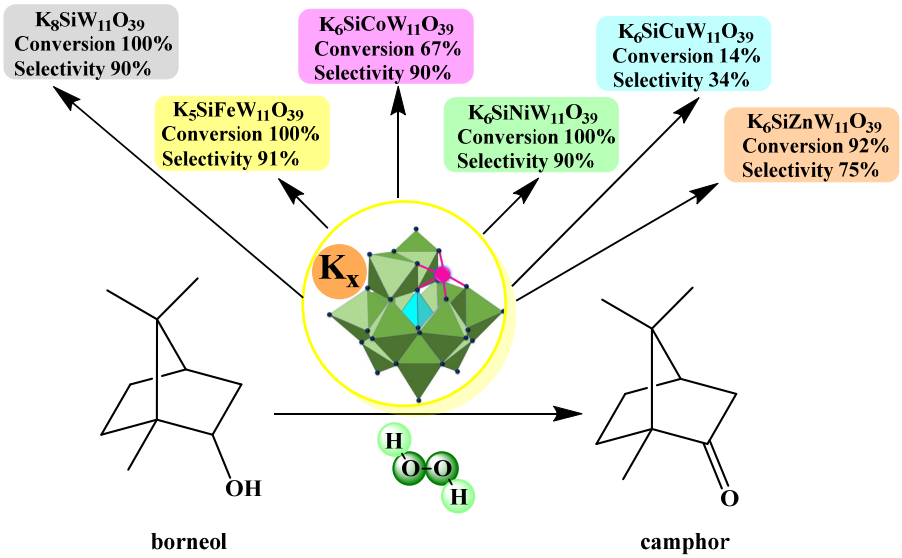

Figure 15. Conversions and selectivity achieved on the borneol oxidation with hydrogen peroxide over transition metal cations -doped potassium silicotungstate salts (adapted from ref. [42]).

Another successful example of metal-doped Keggin HPA potassium salts was described by da Silva et al., which assessed their use in benzaldehyde oxidation reactions with hydrogen peroxide [43]. Scheme 14 describes the yield of benzoic acid achieved in the reactions with various metal-doped catalysts.

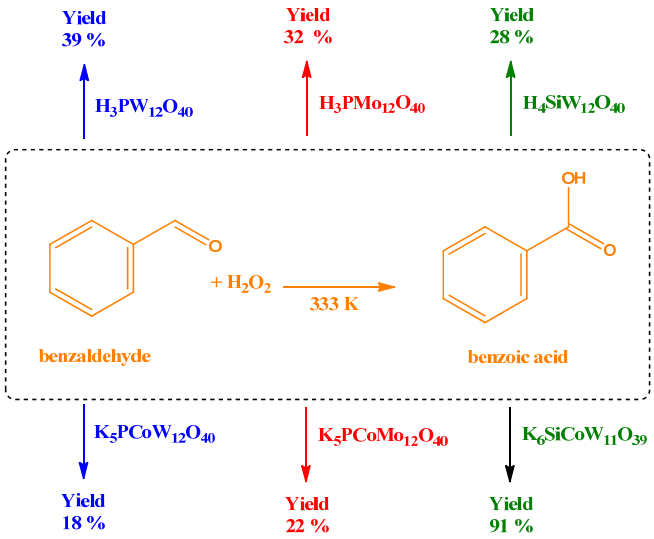

Scheme 14. Benzaldehyde oxidation with hydrogen peroxide over Keggin HPAs or their cobalt-doped Keggin HPA potassium salts (adapted from ref. [43]).

A noticeable result is that in general, the yields achieved in the reactions with the Keggin HPAs or cobalt-doped potassium salts were poor, varying from 18 to 39%, being reaction yields with cobalt salts lower than pristine HPAs. The remarkable exception was the $K_6SiW_{11}CoO_{39}$-catalyzed reaction, which achieved the highest yield (i.e., 91%) [43].

Da Silva et al. investigated the oxidation of benzylic alcohol with hydrogen peroxide over metal-doped phosphotungstic acid potassium salts [30]. Figure 16 displays the main results.

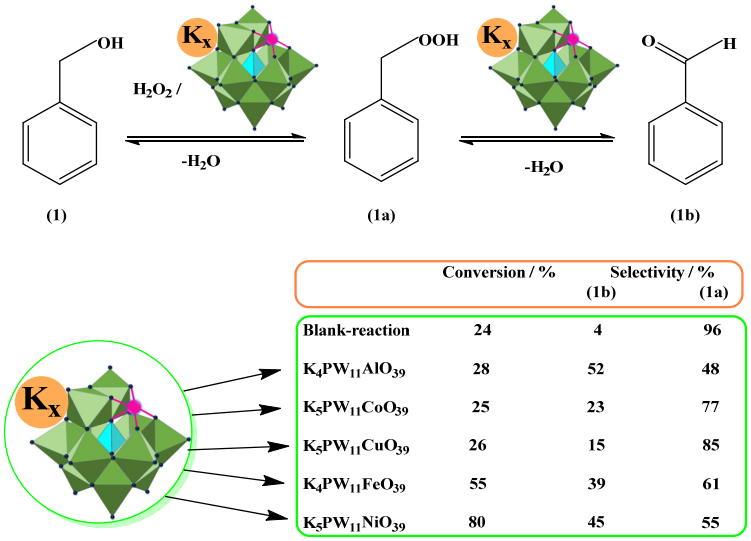

	Conversion / %	Selectivity / % (1b)	Selectivity / % (1a)
Blank-reaction	24	4	96
$K_4PW_{11}AlO_{39}$	28	52	48
$K_5PW_{11}CoO_{39}$	25	23	77
$K_5PW_{11}CuO_{39}$	26	15	85
$K_4PW_{11}FeO_{39}$	55	39	61
$K_5PW_{11}NiO_{39}$	80	45	55

Figure 16. Benzylic alcohol oxidation with hydrogen peroxide over aluminium or transition metal-doped lacunar phosphotungstic acid potassium salts (adapted from ref. [30].

Different than found in the benzaldehyde oxidation [43], where the cobalt-doped potassium phosphotungstate salt was the most active catalyst, herein, the reactions carried out over the nickel-doped potassium phosphotungstate salt were those that achieved the highest conversion and selectivity to carboxylic alcohol (benzylic acid) [30]. Patel et al. have found a similar result, where nickel-doped phosphotungstic acid salt was the most efficient catalyst in oxidation reactions of aldehydes and alcohols, however, those authors used the catalyst supported on the zirconia [44].

Serwicka et al. investigate the Keggin salts in Baeyer Villiger oxidation of cyclohexanone [12]. Partially exchanged salts with cobalt, manganese, or iron cations were the catalysts (Figures 17 and 18).

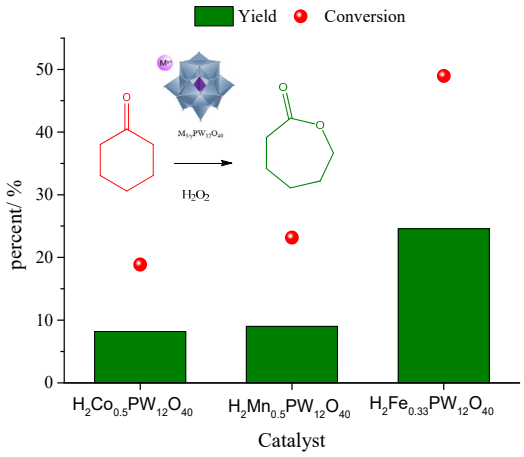

Figure 17. Baeyer Villiger oxidation of cyclohexanone with hydrogen peroxide over partially exchanged-phosphotungstic acid salts (adapted from ref. [12]).

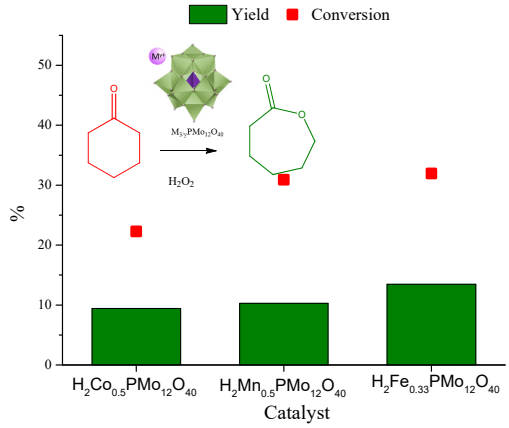

Figure 18. Baeyer Villiger oxidation of cyclohexanone with hydrogen peroxide over partially exchanged-phosphomolybdic acid salts (adapted from ref. [12]).

Among the evaluated salts, it is possible to observe that while the reactions in the presence of cobalt or manganese salts achieved almost the same conversion and selectivity, regardless of Keggin anion, the reactions with iron as the dopant were the most efficient (Figures 17 and 18). However, the $H_2Fe_{0\cdot33}PW_{12}O_{40}$-catalyzed reaction achieved the highest conversion and lactone selectivity if compared to the reaction in the presence of $H_2Fe_{0\cdot33}PMo_{12}O_{40}$ [43].

The performance of silicotungstic acid and its saturated or lacunar salts of *tert*-butylammonium was evaluated in the oxidation reaction of cyclopentene [45]. Scheme 15 shows the main results of conversion and selectivity. Cyclopentene was selectively converted to cyclopentanediol and 1,5-diketone.

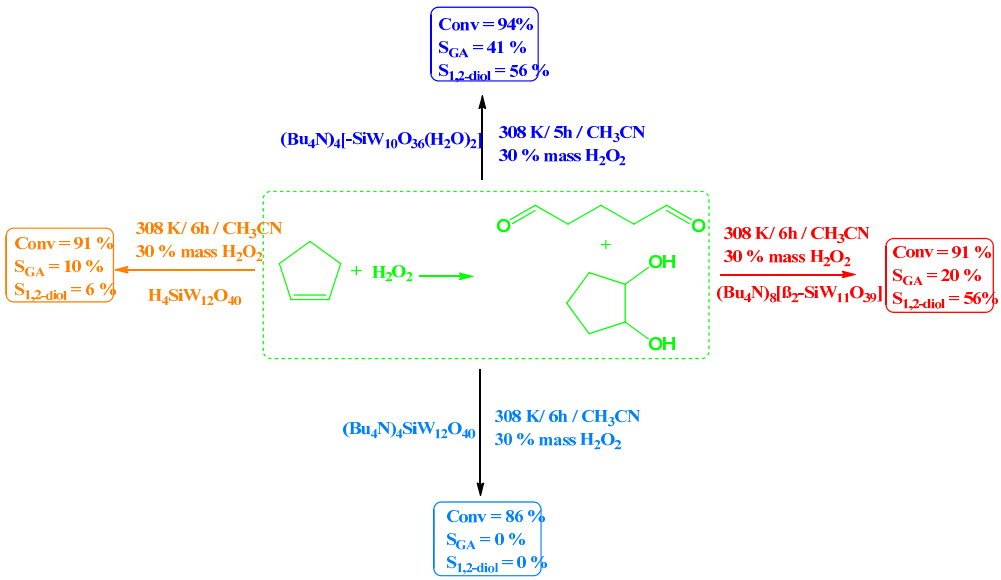

Scheme 15. Conversion and selectivity of silicotungstate-catalyzed oxidation of cyclopentene with hydrogen peroxide (adapted from ref. [45]) [a,b]. [a] Reaction conditions, catalyst (0.03 mmol), CH_3CN (4 mL), cyclopentene (25 mmol), H_2O_2 (30% (mass)) 30 mmol); stirring speed: 500 r·min^{-1}. [b] Conversions and selectivity values were expressed only with one or two significant figures.

All the silicotungstate salts were very efficient catalysts, except the tert-butylammonium silicotungstate saturated salt. Once more the importance of the presence of a vacancy on the Keggin structure of heteropolyanions was demonstrated. Although the silicotungstic acid had achieved a high conversion, the selectivity to oxidation products was poor. The performance of di-lacunar salt was superior to the mono-lacunar silicotungstate.

Tahar et al. prepared nickel or ammonium salts of phosphomolybdic acid replacing partially their protons and evaluated its catalytic activity in reactions of oxidative cleavage of cyclohexanone to adipic acid [46]. Nickel performance is depicted in Schemes 16 and 17.

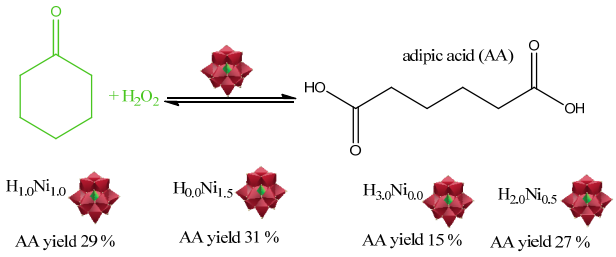

Scheme 16. Partially exchanged acid phosphomolybdic acid nickel salts as catalysts in oxidative cleavage of cyclohexanone to give adipic acid (adapted from ref. [45]).

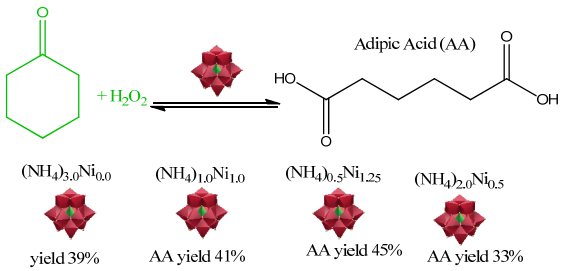

Scheme 17. Partially Ni-exchanged ammonium phosphomolybdate salts as catalysts in oxidative cleavage of cyclohexanone to give adipic acid (adapted from ref. [46]).

Those authors verified that 14 h was time enough to achieve a good conversion. They investigated the effect of catalyst load, and the main results are in Scheme 18.

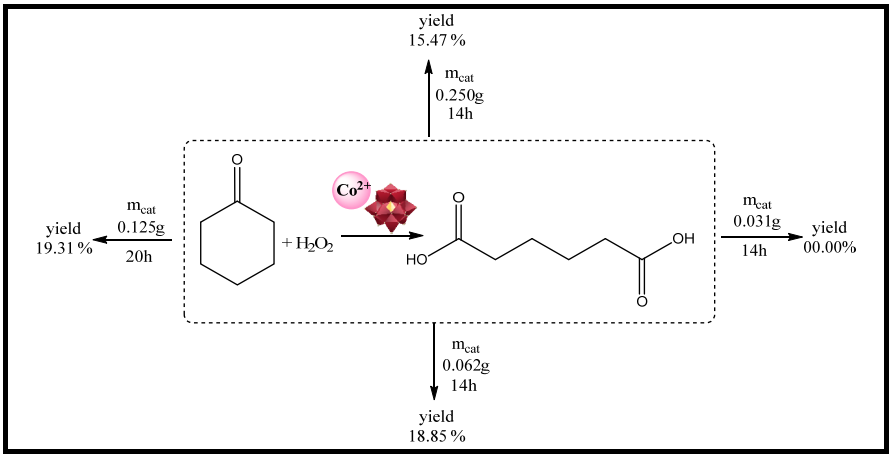

Scheme 18. Effect of catalyst load on the oxidative cleavage of cyclohexanone to adipic acid over nickel phosphomolybdate salts (adapted from ref. [46]).

5. Conclusions

The synthesis routes of a series of Keggin heteropolyacid (HPAs) salts were described. Infrared, powder XRD patterns and measurements of the acidity strength of these salts were discussed. The Keggin HPA salt catalysts are used in the oxidation processes of monoterpenes, aldehydes, alcohols, and olefines to produce valuable fine chemicals. Herein, the most significant results were described. Lacunar HPA salts and metal-doped HPA salts were the focus and had their activity compared in several oxidative processes. A comparison of the main results of these two types of processes showed that the Keggin heteropolyacid salts are efficient catalysts, with performance superior to the conventional

catalysts used in oxidation processes, either with hydrogen peroxide or molecular oxygen. Commonly, noble metal catalysts such as Au, Ag, and Pd are used in oxidation processes. However, they decompose hydrogen peroxide and are incompatible with this oxidant. Even when used with molecular oxygen, frequently they require high oxygen pressure, hampering the processes. Therefore, Keggin HPA salts are efficient and cheaper than these noble metals. Moreover, hydrogen peroxide is a nonflammable oxidant and easier to handle than molecular oxygen.

Author Contributions: Conceptualization, M.J.d.S.; methodology, M.J.d.S.; software, M.J.d.S., N.P.G.L. and A.A.R.; investigation, M.J.d.S., N.P.G.L. and A.A.R.; resources, M.J.d.S., N.P.G.L. and A.A.R.; writing—original draft preparation, M.J.d.S.; writing—review and editing, M.J.d.S.; supervision, M.J.d.S. All authors have read and agreed to the published version of the manuscript.

Funding: Aperfeiçoamento de Pessoal de Nível Superior—Brasil (CAPES—Finance Code 001).

Data Availability Statement: Not applicable.

Acknowledgments: The authors are grateful to the Brazilian research agencies, CAPES, FAPEMIG and CNPq for the financial support.

Conflicts of Interest: The authors declare no conflict of interest.

References

1. Robinson, A.M.; Hensley, J.E.; Medlin, J.W. Bifunctional Catalysts for Upgrading of Biomass-Derived Oxygenates: A Review. *ACS Catal.* **2016**, *6*, 5026–5043. [CrossRef]
2. Tang, C.; Cheng, Y.; Min, X.; Jiang, S.P.; Wang, S. Bifunctional Catalysts for Reversible Oxygen Evolution Reaction and Oxygen Reduction Reaction. *Chem. Eur. J.* **2020**, *26*, 3906–3929. [CrossRef]
3. Tan, K.B.; Zhan, G.; Sun, D.; Huang, J.; Li, Q. The development of bifunctional catalysts for carbon dioxide hydrogenation to hydrocarbons via the methanol route: From a single component to integrated components. *J. Mater. Chem. A* **2021**, *9*, 5197–5231. [CrossRef]
4. Stamenkovic, V.R.; Mun, B.S.; Arenz, M.; Mayrhofer, K.J.; Lucas, C.A.; Wang, G.; Ross, P.N.; Markovic, N.M. Trends in electrocatalysis on extended and nanoscale Pt-bimetallic alloy surfaces. *Nat. Mater.* **2007**, *6*, 241–247. [CrossRef] [PubMed]
5. Fu, Q.; Saltsburg, H.; Flytzani-Stephanopoulos, M. Active nonmetallic Au and Pt species on ceria-based water-gas shift catalysts. *Science* **2003**, *301*, 935–938. [CrossRef]
6. Robinson, A.M.; Ferguson, G.A.; Gallagher, J.R.; Cheah, S.; Beckham, G.T.; Schaidle, J.A.; Hensley, J.E.; Medlin, J.W. Enhanced Hydrodeoxygenation of m-Cresol over Bimetallic Pt–Mo Catalysts through an Oxophilic Metal-Induced Tautomerization Pathway. *ACS Catal.* **2016**, *6*, 4356–4368. [CrossRef]
7. Suntivich, J.; May, K.J.; Gasteiger, H.A.; Goodenough, J.B.; Shao-Horn, Y. A Perovskite Oxide Optimized for Oxygen Evolution Catalysis from Molecular Orbital Principles. *Science* **2011**, *334*, 1383–1385. [CrossRef]
8. Fu, Q.; Deng, W.; Saltsburg, H.; Flytzani-Stephanopoulos, M. Activity and stability of low-content gold–cerium oxide catalysts for the water–gas shift reaction. *Appl. Catal. B* **2005**, *56*, 57–68. [CrossRef]
9. Yoshida, K.; Inokuma, T.; Takasu, K.; Takemot, Y. Catalytic Asymmetric Synthesis of Both Enantiomers of 4-Substituted 1,4-Dihydropyridines with the Use of Bifunctional Thiourea-Ammonium Salts Bearing Different Counterions. *Molecules* **2010**, *15*, 8305–8326. [CrossRef]
10. Villa-Marcos, B.; Li, C.; Mulholland, K.R.; Hogan, P.J.; Xiao, J. Bifunctional Catalysis: Direct Reductive Amination of Aliphatic Ketones with an Iridium-Phosphate Catalyst. *Molecules* **2010**, *15*, 2453–2472. [CrossRef]
11. Amaya, J.; Moreno, S.; Molina, R. Heteropolyacids supported on clay minerals as bifunctional catalysts for the hydroconversion of decane. *Appl. Cat. B Environ.* **2021**, *297*, 120464–120479. [CrossRef]
12. Pamin, K.; Połtowicz, J.; Pronczuk, M.; Krysciak-Czerwenka, J.; Karcz, R.; Serwick, E.M. Keggin-Type Heteropoly Salts as Bifunctional Catalysts in Aerobic Baeyer-Villiger Oxidation. *Materials* **2018**, *11*, 1208. [CrossRef] [PubMed]
13. Kirpsza, A.; Lalik, E.; Mordarski, G.; Micek-Ilnicka, A. Catalytic properties of carbon nanotubes-supported heteropolyacids in isopropanol conversion. *Appl. Catal. A* **2018**, *549*, 254–262. [CrossRef]
14. Kozhevnikov, I.V. Heteropoly acids and related compounds as catalysts for fine chemical synthesis. *Catal. Rev.* **1995**, *37*, 311–352. [CrossRef]
15. Balbinot, L.; Schuchardt, U.; Vera, C.; Sepulveda, J. Oxidation of cyclohexanol to epsilon-caprolactone with aqueous hydrogen peroxide on $H_3PW_{12}O_{40}$ and $Cs_{2.5}H_{0.5}PW_{12}O_{40}$. *Catal. Commun.* **2008**, *9*, 1878–1881. [CrossRef]
16. Yang, Z.W.; Xu, X.Q.; Li, T.J.; Zhang, N.N.; Zhao, X.; Chen, W.L.; Liang, X.X.; He, X.L.; Ma, H.C. Preparation and Catalytic Property of Multi-walled Carbon Nanotubes Supported Keggin-Typed Tungstosilicic Acid for the Baeyer-Villiger Oxidation of Ketones. *Catal. Lett.* **2015**, *145*, 1955–1960. [CrossRef]

17. Karaman, B.P.; Oktar, N.; Doğu, G.; Dogu, T. Heteropolyacid Incorporated Bifunctional Core-Shell Catalysts for Dimethyl Ether Synthesis from Carbon Dioxide/Syngas. *Catalysts* **2022**, *12*, 1102. [CrossRef]
18. Narkhede, N.; Patel, A. Efficient synthesis of biodiesel over a recyclable catalyst comprising a monolacunary silicotungstate and zeolite Hβ. *RSC Adv.* **2014**, *4*, 64379–64387. [CrossRef]
19. Ma, Q.G.; Zhao, J.R.; Xing, W.Z.; Peng, X.H. Baeyer-Villiger Oxidation of Cyclic Ketones Using Aqueous Hydrogen Peroxide Catalyzed by Heteropolyacids in Solvent-free System. *J. Adv. Oxid. Technol.* **2014**, *17*, 212–216. [CrossRef]
20. Deutsch, J.; Martin, A.; Lieske, H. Investigation on heterogeneously catalyzed condensation of glycerol to cyclic acetals. *J. Catal.* **2007**, *245*, 428–435. [CrossRef]
21. Pizzio, L.R.; Blanco, M.N. A contribution to the physicochemical characterization of nonstoichiometric salts of tungstosilicic acid. *Microporous Mesoporous Mater.* **2007**, *103*, 40–47. [CrossRef]
22. Dias, J.A.; Caliman, E.; Dias, S.C.L. Effects of cesium ion exchange on the acidity of 12-tungstophophoric acid. *Microporous Mesoporous Mater.* **2004**, *76*, 221–232. [CrossRef]
23. Díaz, J.; Pizzio, L.R.; Pecchi, G.; Campos, C.H.; Azócar, L.; Briones, R.; Romina Romero, R.; Henríquez, A.; Gaigneaux, E.M.; Contreras, D. Tetrabutyl Ammonium Salts of Keggin-Type Vanadium-Substituted Phosphomolybdates and Phosphotungstates for Selective Aerobic Catalytic Oxidation of Benzyl Alcohol. *Catalysts* **2022**, *12*, 507. [CrossRef]
24. Da Silva, M.J.; Lopes, N.P.G.; Ferreira, S.O.; Da Silva, R.C.; Natalino, R.; Chaves, D.M.; Texeira, M.G. Monoterpenes etherification reactions with alkyl alcohols over cesium partially exchanged Keggin heteropoly salts: Effects of the catalyst composition. *Chem. Pap.* **2021**, *75*, 153–168. [CrossRef]
25. Park, H.W.; Park, S.; Park, D.R.; Choi, J.H.; Song, I.K. Decomposition of phenethyl phenyl ether to aromatics over $Cs_xH_{3\cdot 0-x}PW_{12}O40$ (X= 2.0–3.0) heteropolyacid catalysts. *Catal. Commun.* **2010**, *12*, 35. [CrossRef]
26. Vilanculo, C.B.; Da Silva, M.J. Unraveling the role of the lacunar $Na_7PW_{11}O_{39}$ catalyst on the oxidation of terpene alcohols with hydrogen peroxide at room temperature. *New J. Chem.* **2020**, *44*, 2813–2820. [CrossRef]
27. Da Silva, M.J.; Rodrigues, A.A. Metal silicotungstate salts as catalysts in furfural oxidation reactions with hydrogen peroxide. *Mol. Catal.* **2020**, *493*, 111104–111114. [CrossRef]
28. Vilanculo, C.B.; Da Silva, M.J.; Ferreira, S.O.; Teixeira, M.G. A rare oxidation of camphene to acid and aldehyde in the presence of Lacunar Keggin heteropoly salts. *Mol. Catal.* **2019**, *478*, 110589–110596. [CrossRef]
29. Vilanculo, C.B.; Da Silva, M.J.; Teixeira, M.G.; Villarreal, J.A. One-pot synthesis at room temperature of epoxides and linalool derivative pyrans in monolacunary $Na_7PW_{11}O_{39}$-catalyzed oxidation reactions by hydrogen peroxide. *RSC Adv.* **2020**, *10*, 7691–7697. [CrossRef]
30. Coronel, N.C.; Da Silva, M.J.; Ferreira, S.O.; Da Silva, R.C.; Natalino, R. $K_5PW_{11}NiO_{39}$-catalyzed oxidation of benzyl alcohol with hydrogen peroxide. *Chem. Select.* **2019**, *4*, 302–310. [CrossRef]
31. Rocchiccioli-Deltcheff, C.; Fournier, M. Catalysis by polyoxometalates. Part 3—Influence of Vanadium(V) on the thermal stability of 12-metallophosphoric acids from in situ infrared studies. *J. Chem. Soc. Faraday Trans.* **1991**, *87*, 3913–3920. [CrossRef]
32. Mansilla, D.S.; Torviso, M.R.; Alesso, E.N.; Vazquez, P.G.; Caceres, C.V. Synthesis and characterization of copper and aluminium salts of H3PMo12O40 for their use as catalysts in the eco-friendly synthesis of chromanes. *Appl. Catal. A* **2010**, *375*, 196–204. [CrossRef]
33. Pathan, S.; Patel, A.; Tilani, H. Selective Oxidation of Alcohols and Alkenes with Molecular Oxygen Catalyzed by Highly Dispersed Cobalt (II) Decorated 12-Tungstosilicic Acid-Modified Zirconia. *Catalysts* **2022**, *12*, 1622. [CrossRef]
34. Da Silva, M.J.; Leles, L.C.A.; Teixeira, M.G. Lewis acid metal cations exchanged heteropoly salts as catalysts in β-pinene etherification. *React. Kinet. Mech. Catal.* **2020**, *131*, 875–887. [CrossRef]
35. Da Silva, M.J.; Leles, L.C.A.; Ferreira, S.O.; Da Silva, R.C.; Viveiros, K.d.V.; Chaves, D.M.; Pinheiro, P.F. A Rare Carbon Skeletal Oxidative Rearrangement of Camphene Catalyzed by Al-Exchanged Keggin Heteropolyacid Salts. *ChemSelect* **2019**, *4*, 7665–7672. [CrossRef]
36. Patel, A.; Patel, J. Nickel salt of phosphomolybdic acid as a bi-functional homogeneous recyclable catalyst for the base free transformation of an aldehyde into ester. *RSC Adv.* **2020**, *10*, 22146–22155. [CrossRef]
37. Patel, A.; Patel., J. Exchanged Supported Phosphomolybdic Acid: Synthesis, Characterization and Low-Temperature Water Mediated Hydrogenation of Cyclohexene. *Catal. Lett.* **2022**, *152*, 2716–2728. [CrossRef]
38. Mizuno, N.; Misono, M.; Okuhara, T. Catalytic Chemistry of Heteropoly Compounds. *Adv. Catal.* **1996**, *41*, 113–252. [CrossRef]
39. Méndez, L.; Torviso, R.; Pizzio, L.; Blanc, M. 2-Methoxynaphthalene acylation using aluminium or copper salts of tungstophosphoric and tungstosilicic acids as catalysts. *Catal. Today* **2011**, *173*, 32–37. [CrossRef]
40. Shringarpure, P.; Patel, A. Cobalt (II) exchanged supported 12-tungstophosphoric acid: Synthesis, characterization, and non-solvent liquid phase aerobic oxidation of alkenes. *J. Mol. Catal. A* **2010**, *321*, 22–26. [CrossRef]
41. Karcz, R.; Niemiec, P.; Pamin, K.; Połtowicz, J.; Kryściak-Czerwenka, J.; Napruszewska, B.D.; Michalik-Zym, A.; Witko, M.; Tokarz-Sobieraj, R.; Serwicka, E.M. Effect of cobalt location in Keggin-type heteropoly catalysts on aerobic oxidation of cyclooctane: Experimental and theoretical study. *Appl. Catal. A* **2017**, *542*, 317–326. [CrossRef]
42. Da Silva, M.J.; Andrade, P.H.S.; Sampaio, V.F.C. Transition metal-substituted potassium silicotungstate salts as catalysts for oxidation of terpene alcohols with hydrogen peroxide. *Catal. Lett.* **2021**, *151*, 2094–2106. [CrossRef]
43. Da Silva, M.J.; Leles, L.C.A.; Natalino, R.; Ferreira, S.O.; Coronel, N.C. An efficient benzaldehyde oxidation by hydrogen peroxide over metal-substituted lacunary Potassium heteropolyacid Salts. *Catal. Lett.* **2018**, *148*, 1202–1214. [CrossRef]

44. Patel, A.; Patel, A. Nickel exchanged supported 12-tungstophosphoric acid: Synthesis, characterization and base free one-pot oxidative esterification of aldehyde and alcohol. *RSC Adv.* **2019**, *9*, 1460–1471. [CrossRef] [PubMed]
45. Chen, P.; Fang, Y.; Xie, K.; Chen, Y.; Liu, Y.; Zuo, H.; Lu, W.; Liu, B. Lacunary silicotungstic heteropoly salts as high-performance catalysts in the oxidation of cyclopentene. *Chin. J Eng. Chem.* **2022**, *56*, 152–159. [CrossRef]
46. Tahar, A.; Benadji, S.; Mazari, T.; Dermeche, L.; Marchal-Roch, C.; Rabia, C. Preparation, Characterization and Reactivity of Keggin Type Phosphomolybdates, $H_{3-2x}Ni_xPMo_{12}O_{40}$ and $(NH_4)_{3-2x}$ $Ni_xPMo_{12}O_{40}$, for Adipic Acid Synthesis. *Catal Lett.* **2015**, *145*, 569–575. [CrossRef]

Disclaimer/Publisher's Note: The statements, opinions and data contained in all publications are solely those of the individual author(s) and contributor(s) and not of MDPI and/or the editor(s). MDPI and/or the editor(s) disclaim responsibility for any injury to people or property resulting from any ideas, methods, instructions or products referred to in the content.